Research Square

Preprints are preliminary reports that have not undergone peer review.
They should not be considered conclusive, used to inform clinical practice,
or referenced by the media as validated information.

Mechanical Behavior and Stabilization Mechanisms of Loess Modified by Guar Gum and Nano-SiO_2 Composites

Zhao Duan
Xi'an University of Science and Technology
Shunxin Zhang
zhangsx157@stu.xust.edu.cn
Xi'an University of Science and Technology
Xinyan Xie
Shaanxi Institute of Engineering Prospecting Co., Ltd
Zhe Yang
China Coal xi'an Design Engineering Co., Ltd
Zhuo Nan
Shaanxi Tiandi Geology Co., Ltd

Article

Keywords: Modified loess, Guar gum, Nano-SiO2, Mechanical behavior, Slaking resistance, Stabilization mechanisms

Posted Date: November 18th, 2026

DOI: https://doi.org/10.21203/rs.3.rs-11596928/v1

License: This work is licensed under a Creative Commons Attribution 4.0 International License.
Read Full License

Additional Declarations: No competing interests reported.

Mechanical Behavior and Stabilization Mechanisms of Loess Modified by Guar Gum and Nano-SiO_2 Composites

Zhao Duan[a]
[a] College of Geology and Environment, Xi'an University of Science and Technology, Xi'an 710054, China; email: duanzhao@xust.edu.cn

Shunxin Zhang[a*]
[a] College of Geology and Environment, Xi'an University of Science and Technology, Xi'an 710054, China
*Corresponding author: +86 157 6928 5572; email: zhangsx157@stu.xust.edu.cn;
address: 58 Yanta Middle Road, Xi'an 710054, China

Xinyan Xie[b]
[b] Shaanxi Institute of Engineering Prospecting Co., Ltd, Xi'an 710054, China; email: 1282242945@qq.com

Zhe Yang [c]
[c] China Coal xi'an Design Engineering Co., Ltd, Xi'an 710054, China; email: yangzhe1@chinacoal.com

Zhou Nan[d]
[d] Shaanxi Tiandi Geology Co., Ltd, Xi'an 710054, China; email: nan6262626@163.com

Manuscript to be submitted to

Scientific Reports

2 November 2026

Mechanical Behavior and Stabilization Mechanisms of Loess Modified by Guar Gum and Nano-SiO_2 Composites

Zhao Duan; **Shunxin Zhang**; **Xinyan Xie; Zhe Yang; Zhuo Nan**

Abstract

Enhancing loess strength, reducing collapsibility, and improving foundation bearing capacity are essential for ensuring durable infrastructure in loess regions. This study evaluated Middle Pleistocene (Q_2) loess from the Jingyang South Tableland modified with guar gum (GG) and nano-SiO_2 (NS). Direct shear tests, slaking tests, basic physical-property tests, and scanning electron microscopy (SEM) observations were systematically conducted to assess the effects of modifier content on mechanical behavior and slaking resistance. Both modifiers increased loess shear strength, and GG more effectively improved slaking resistance. Among the single-modifier treatments, 1.0% GG and 2.5% NS produced the optimal overall performance. SEM revealed that GG established a three-dimensional cementation network linking soil particles, while NS primarily filled micropores. Furthermore, the GG–NS composite enhanced shear strength more substantially than either modifier alone, whereas its slaking resistance surpassed that of NS-modified loess but remained inferior to that of GG-modified loess. GG and NS exhibited both synergistic and counteracting effects governed by their content and blending ratio, with the 1.0% GG + 2.5% NS achieving the best overall performance. These findings elucidate the stabilization mechanisms of biopolymer–nanomaterial composite-modified loess and provide practical insights for geotechnical engineering in loess terrains.

Keywords: Modified loess; Guar gum; Nano-SiO_2; Mechanical behavior; Slaking resistance; Stabilization mechanisms

1. **Introduction**

As a Quaternary aeolian deposit, loess is widely distributed across China, covering an approximate area of 6.4×10^5 km^2 [1]. However, loess is inherently characterized by high porosity, weak interparticle cementation, and severe water sensitivity [2, 3]. In particular, compacted loess—a commonly used earthwork material in northern China—frequently suffers engineering geological hazards induced by water infiltration during infrastructure development, such as differential foundation settlement [4, 5], embankment slope failure [6, 7], and check dam instability [8]. Consequently, to effectively enhance the engineering properties of loess, chemical and biological modification methods have been widely adopted owing to their cost-effectiveness, operational simplicity, and remarkable performance [9].

With the continuous advancement of materials science, traditional soil modification materials, such as lime, cement, and fly ash, are increasingly being supplemented or replaced by novel modifiers [10]. Among them, biopolymers are recognized as highly promising soil modification materials owing to their environmental friendliness, cost-effectiveness, and widespread availability [11]. Among various biopolymers, guar gum (GG) has exhibited a pronounced effect on soil modification [12-14].

Concurrently, nanomaterials have garnered widespread attention as particulate soil modification materials. Nanomaterials are defined as materials or their composites possessing at least one external dimension not exceeding 100 nm, exhibiting unique characteristics such as ultrafine particle sizes, high specific surface areas, and pronounced surface reactivity [15]. Nano-SiO_2 (NS), a representative nanomaterial, possesses favorable attributes including abundant raw reserves, green and efficient preparation processes, and environmentally friendly [16].

Presently, research on soil modification has shifted from single additives toward multi-component composite materials. Capitalizing on the performance merits of various modifiers, researchers have conducted extensive investigations into soil modification using composite agents. Studies on the mechanical strength characteristics of different modified soils indicate that GG and NS exhibit comparable modification efficacy: incorporating low modifier contents into the soil markedly enhances its mechanical strength, whereas further increases in modifier content attenuate this enhancement [17-19]. Compared to single modifiers, composite modifiers demonstrate pronounced

mechanical synergy [20-23]. Regarding water stability modification, GG significantly reduces soil permeability and improves soil water stability through cementation and adsorption [24]. In contrast, NS enhances the water stability of modified soil primarily at elevated contents, where numerous fine soil particles are adsorbed onto the surfaces of coarse particles under the influence of NS, generating substantial micro-aggregates [25]. The effectiveness of composite modifiers in improving soil water stability is closely related to the properties of their constituent materials [26]. In investigations of the micro-mechanisms governing soil modification, GG and NS demonstrate distinctly contrasting microstructural characteristics. GG interacts with pore water to form gel-like aggregates that occlude pores, while its functional chemical groups bind soil particles together, thereby mitigating soil dispersibility [19]. Conversely, NS occupies ultrafine pore spaces via its nanoscale dimensions, substantially diminishing the pore size within the soil [27]. Nevertheless, a definitive consensus regarding the micro-mechanisms of composite-modified soils remains elusive, as they are inherently contingent upon the specific constituent components of the composites [28-30].

Extant literature indicates that composite materials can effectively combine the advantages of distinct modifiers, and an optimal mixing ratio is paramount to unlocking the individual potential of each additive. Nevertheless, investigations regarding soil modification using composites incorporating biopolymers and nanoparticles remain scarce. Therefore, to evaluate the modification efficacy and underlying mechanisms of GG and NS composite materials on the mechanical properties and slaking resistance of loess, direct shear tests, immersion slaking tests, and microscopic observations were conducted in this study. This study aimed to 1) determine the modification characteristics of GG and NS composite materials on loess shear strength, 2) elucidate the modification characteristics of the composite materials on loess slaking resistance, and 3) uncover the microstructural characteristics and modification mechanisms of loess modified with GG and NS composites. This investigation on composite-modified loess provides valuable engineering guidance for resolving geotechnical construction challenges in loess regions.

2. Materials and Methods

2.1 Materials

The loess used in this study was sampled from the South Jingyang Tableland in Shaanxi Province, China, and is classified as Upper Pleistocene Malan loess. The basic physical parameters of the tested loess are summarized in Table. 1, and its particle-size distribution curve is shown in Fig. 8.

Two types of modifying materials, namely guar gum (GG) and nano-SiO_2 (NS), were employed in this study (Fig. 1a). GG is a milky-white to light-yellow, odorless, tasteless, and nontoxic powder that disperses readily in water to form a high-viscosity colloidal solution. It exhibits a pH of 6.5, a 1% aqueous solution viscosity of 6,000 mPa·s, and a gum content of 83.61%. NS is a spherical, white, odorless, tasteless, and nontoxic powder capable of uniform dispersion in water. It has a pH of 6.5, an average particle diameter of 20 nm, a purity of 99.95%, and a specific surface area of 185 $m^2 \cdot g^{-1}$.

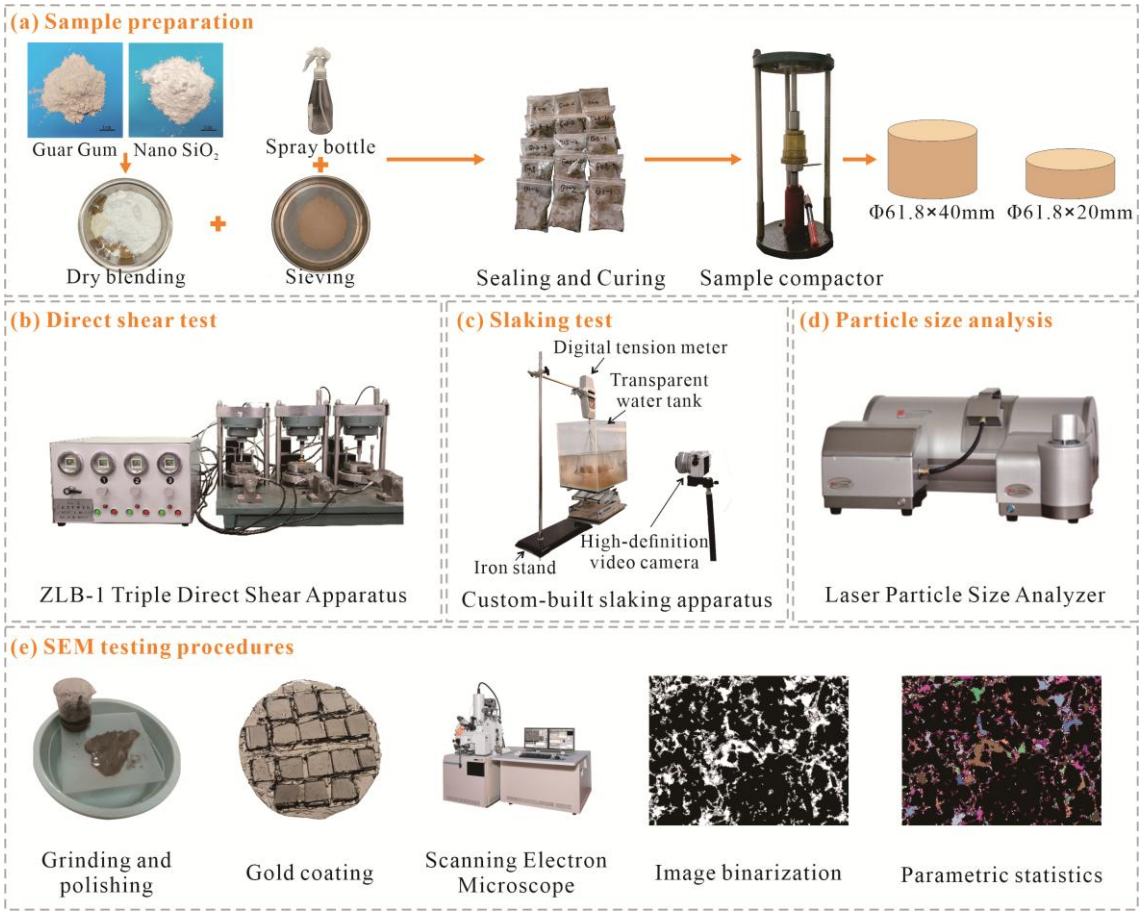


Fig. 1. Specimen Preparation and Testing Apparatus.

2.2 Sample Preparation

The sample preparation procedure in this study complied with relevant ASTM test standards (Fig. 1a).

Based on preliminary trials and prior findings from Kong [27] and Sujatha and Saisree [31], the modifier contents and experimental groups are summarized in Table. 2. The sample preparation involved the following sequential steps: the raw loess was air-dried, crushed, passed through a 2-mm metal sieve, and subsequently oven-dried. The modifiers were then thoroughly blended with the dried loess using a dry-mixing method. The target moisture content of the blended soil mixture was adjusted to 16.0% via a spraying method, after which the mixture was sealed in airtight bags and equilibrated for 24 h. Subsequently, according to specific testing requirements, two sizes of test samples—61.8 mm in diameter by 20 mm in height and 61.8 mm in diameter by 40 mm in height—were fabricated using a multi-layer static compaction method. All test samples were compacted to a controlled dry density of 1.55 g/cm³ and subsequently cured for 7 d.

2.3 Test methods

2.3.1 Direct shear test

Unconsolidated-undrained direct shear tests were conducted using a direct shear apparatus (ZLB-1, Nanjing Soil Instrument Factory Co., Ltd.) on 48 sets of replicate samples with dimensions of 61.8 mm in diameter and 20 mm in height. The shearing rate was controlled at 0.8 mm/min under normal pressure of 100 kPa, 200 kPa, and 400 kPa. The peak shear stress obtained from the shear stress-shear strain curve was taken as the shear strength of the sample. In the absence of an obvious peak, the shear stress corresponding to a shear displacement of 4 mm was defined as the shear strength (Fig. 1b).

2.3.2 Slaking test

Immersion slaking tests were conducted on 16 sets of replicate samples (61.8 mm in diameter and 40 mm in height) using a custom-built slaking apparatus. The apparatus primarily consists of an iron stand, a digital tension meter, a mesh tray, a transparent water tank, and a high-definition video camera (Fig. 1c). The dynamic mass loss of each sample during the slaking process was monitored and recorded via the digital tension gauge. The slaking percentage (H) and slaking velocity (V) can be calculated using equation (1) and (2), respectively:

$$H = \frac{G_o - G_r}{G_0} \times 100\% \quad (1)$$

$$V = \frac{G_o - G_r}{t} \quad (2)$$

where H is the slaking percentage (%); V is the slaking velocity; G_0 is the initial submerged weight of the specimen in the tray (N); G_0 is the remaining weight of the undisintegrated specimen in the tray at time t (N); and t is the slaking time (s).

2.3.3 Basic physical property test

A laser particle size analyzer (Bettersize 2600) (Fig. 1d) was utilized to analyze the samples, during which the obscuration ratio was maintained within 10%–20% to obtain the particle-size distribution curves. Additionally, Atterberg limit tests were performed on the samples using a combined liquid-plastic limit tester. After curing, 16 sets of replicate samples, each measuring 61.8 mm in diameter and 40 mm in height, were crushed and sieved. The resulting material was subsequently used for particle-size analysis and Atterberg limit tests.

2.3.4 Micro-observation test

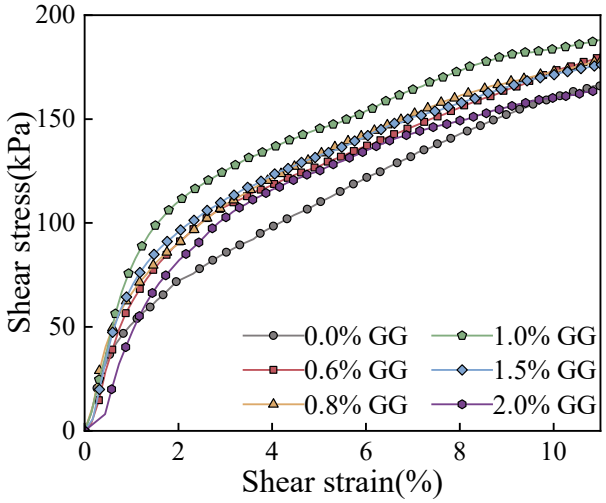
The microstructure of the samples was observed via scanning electron microscopy (JSM-7610F, Japan Electronics Co., Ltd.), SEM micrographs acquired at 500× magnification were selected for comparative analysis (Fig. 1e). Four sets of replicate samples (61.8 mm in diameter and 20 mm in height) were immersed in liquid nitrogen for 1 h and subsequently transferred to a freeze dryer at -50°C for over 24 h to obtain completely dehydrated samples. During SEM sample preparation, a modified syringe was used to extract soil cores along the longitudinal profile of the samples. To ensure uniform infiltration into the soil matrix, an epoxy resin solution was carefully dripped onto the sample surface under a negative pressure generated within the sampler. Once fully cured, the impregnated sample was extruded from the sampler. The sample was then sequentially polished into thin sections using abrasive sandpaper, diamond suspension, and polishing cloth with lubricant. Finally, the surfaces of the thin sections of the SEM samples were sputter-coated with platinum for SEM testing [32].

3. Test Results and Analysis

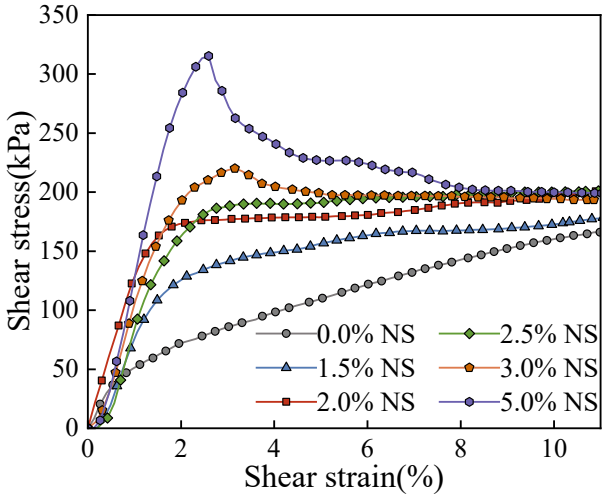
3.1 Shear Strength Characteristics

Direct shear tests were conducted under three normal stresses: 100, 200, and 400 kPa. Owing to space limitations, only the stress–strain curves obtained under a normal stress of 200 kPa are presented herein (Fig. 2). The stress–strain curves of GG-amended loess exhibited strain-hardening behavior

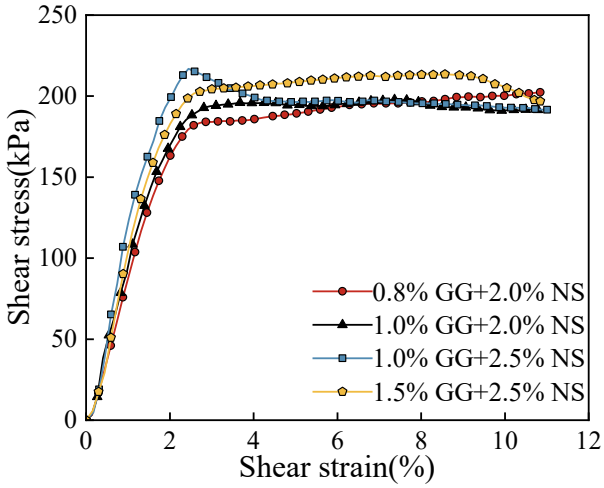
(Fig. 2a), and GG incorporation enhanced the shear strength of the loess. With increasing GG content, the shear strength of the GG-modified loess initially increased and subsequently decreased, reaching a maximum at a GG content of 1% under all three normal-pressure conditions (Fig. 3a). Compared with raw loess, the cohesion of GG-modified loess with GG contents of 0.6%, 0.8%, 1.0%, 1.5%, and 2.0% increased by 42.6%, 55.5%, 88.3%, 54.8%, and 50.1%, respectively, while the corresponding changes in friction angle were 1.3%, 4.9%, 3.8%, 3.7%, and -1.2%, respectively. The effect of GG modification on the cohesion of loess was more pronounced than that on its friction angle (Fig. 4a).



(a)



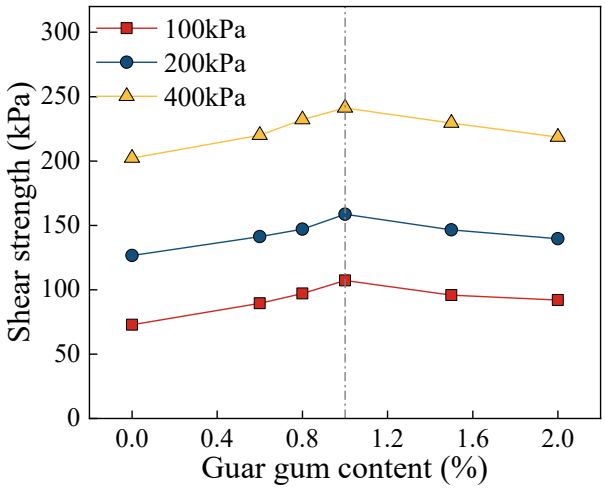
(b)



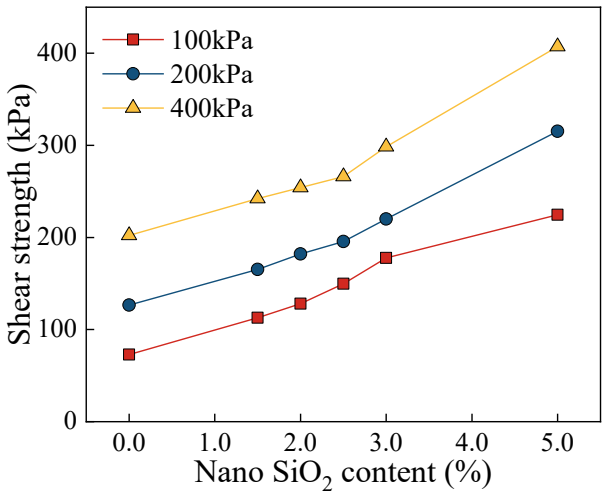
(c)

Fig. 2. Stress-strain curves of loess treated with different modifiers (σ = 200 kPa): (a) GG-modified loess; (b) NS-modified loess; (c) GG+NS composite-modified loess.

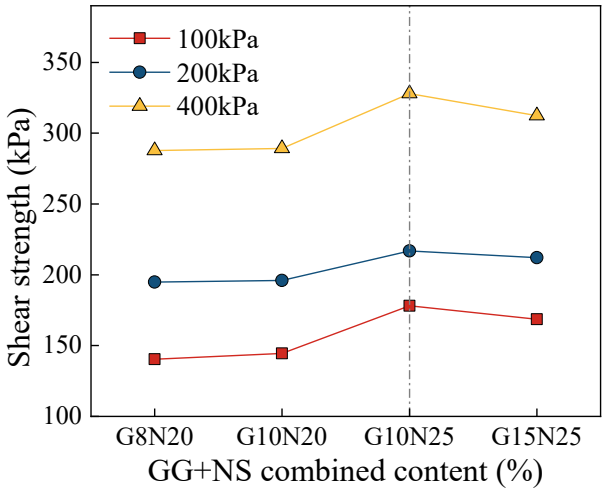
With increasing NS content, the brittle failure characteristics of NS-modified loess became more pronounced (Fig. 2b), while its shear strength and cohesion were substantially enhanced (Fig. 3b and 4b). Compared with raw loess, the cohesion of loess modified with 5% NS increased from 35.05 kPa to 178.63 kPa, representing an increase of 409.6%. In contrast, the friction angle of NS-modified loess exhibited a more complex variation pattern, initially decreasing and then increasing. Overall, NS modification had a more pronounced effect on the cohesion of loess (Fig. 4b).



(a)



(b)

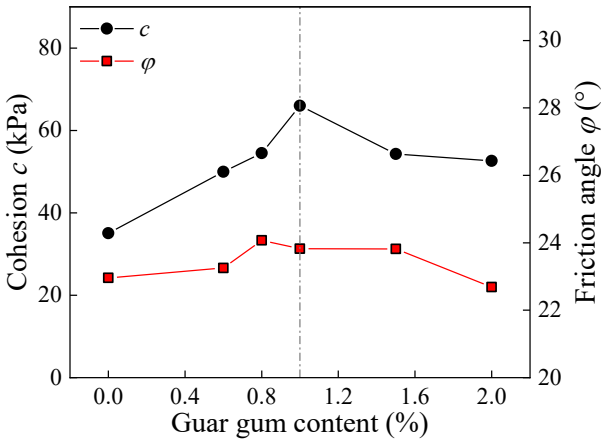


(c)

Fig. 3. Effect of modifier content on the peak shear strength under various normal stresses: (a) GG-modified loess; (b) NS-modified loess; (c) GG+NS composite-modified loess.

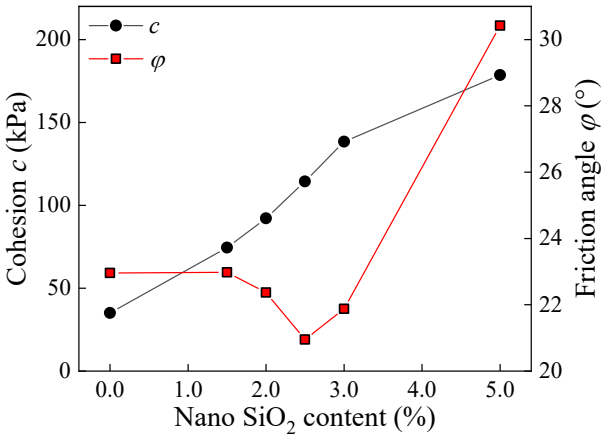
Compared with single modifying materials, the composite modifying material produced a more pronounced enhancement in the shear strength of loess. The shear strength of loess modified with 1.0% GG + 2.5% NS was the highest. Under a normal pressure of 200 kPa, the shear strength of this composite-modified loess was 36.7% and 8.5% higher than that of loess modified with 1.0% GG alone and 2.5% NS alone, respectively (Fig. 3c). As the GG and NS contents in the composite modifying material increased, the cohesion of the modified loess gradually increased, whereas its friction angle showed only minor variation and remained between 25.7° and 26.9° (Fig. 4c). These findings collectively demonstrate that the GG + NS composite exerted the most substantial improvement on

160 loess cohesion.



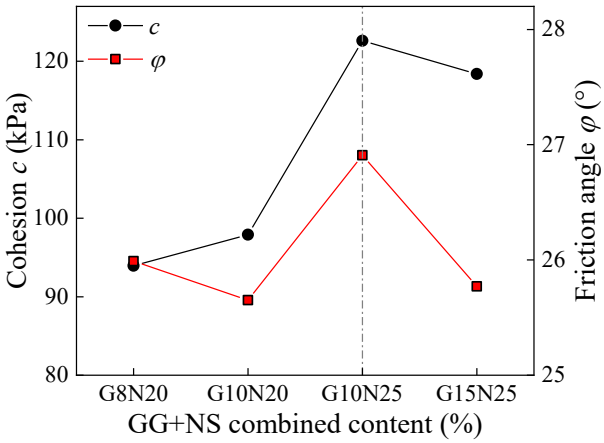
161

162 (a)



163

164 (b)



165

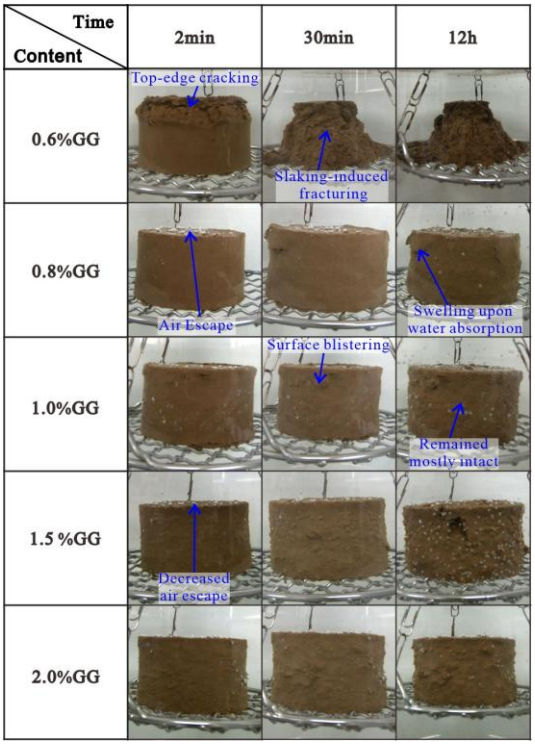
166 (c)

167 **Fig. 4.** Variations in shear strength parameters (c and φ) of modified loess with different modifier

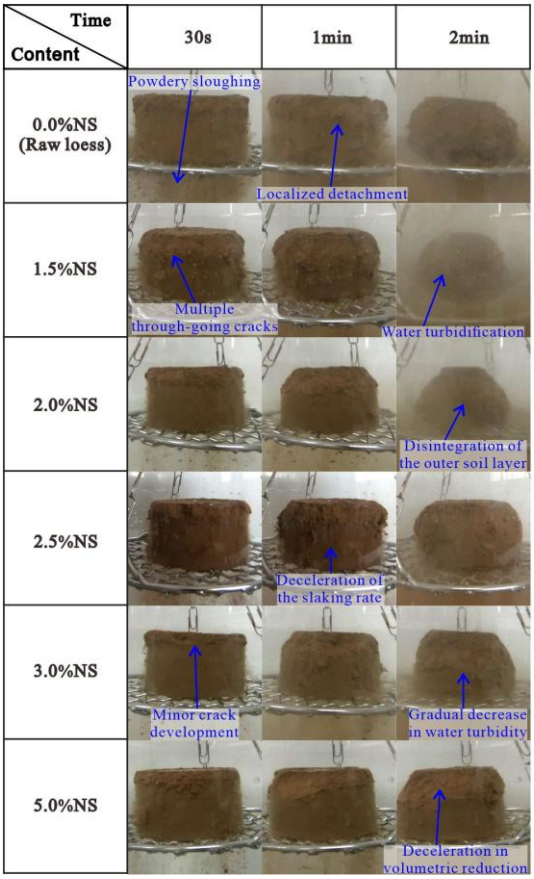
168 contents: (a) GG-modified loess; (b) NS-modified loess; (c) GG+NS composite-modified loess.

3.2 Slaking Resistance Characteristics

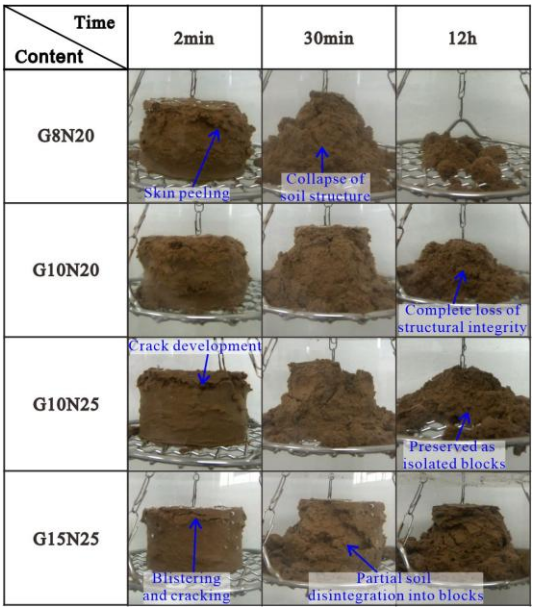
Fig. 5 illustrates the slaking processes of GG-modified loess, NS-modified loess, and GG + NS composite-modified loess. Previous studies by Li [26] and Li [33] reported that the slaking process of raw loess can be divided into three stages: (1) the sample wetting stage (initial stage), during which water infiltrates the soil matrix, inducing the release of numerous air bubbles, while some loess particles detach from the sample as individual particles; (2) the sample softening stage (intermediate stage), during which large fissures develop and portions of the soil detach from the sample; and (3) the complete slaking stage (final stage), during which the slaking rate accelerates until complete slaking occurs. In the present study, the slaking process of raw loess also exhibited these three stages (Fig. 5b).



(a)



(b)

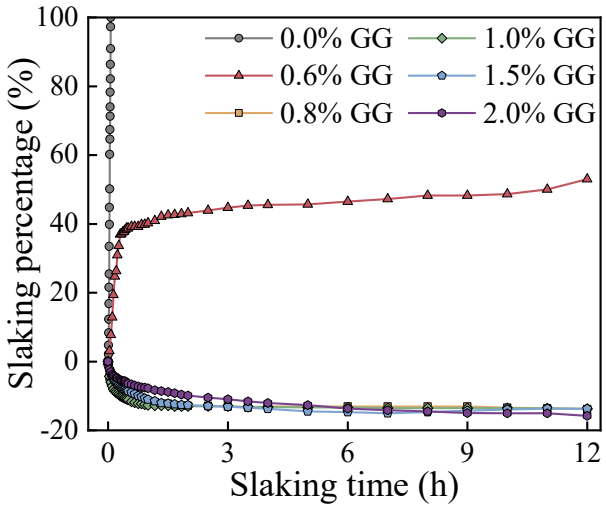


(c)

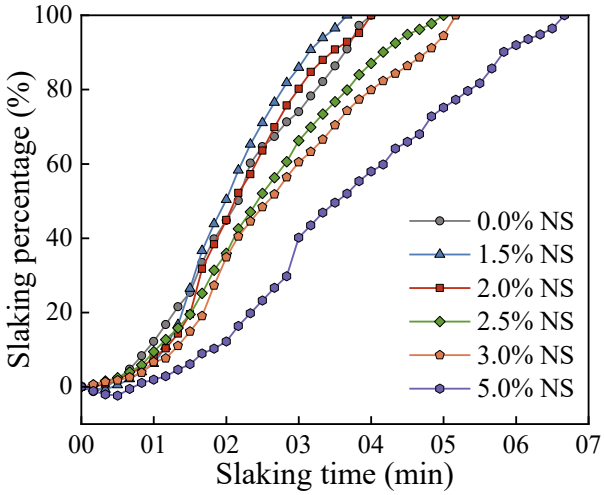
Fig. 5. Slaking process of differently modified loess specimens: (a) GG-modified loess; (b) NS-modified loess; (c) GG+NS composite-modified loess.

As shown in Fig. 5a, GG incorporation significantly improved the slaking resistance of loess.

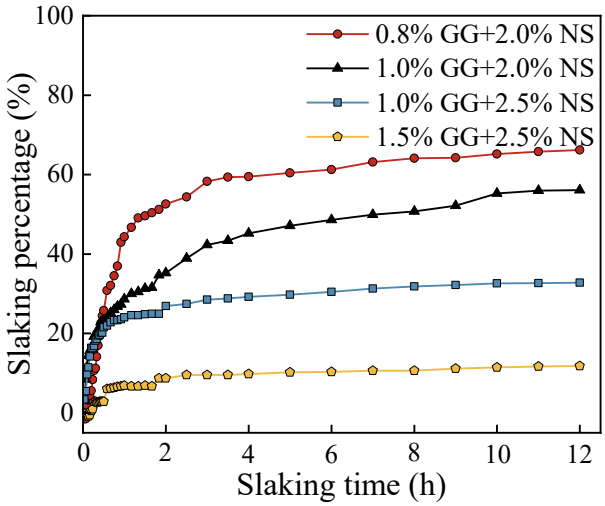
After 12 h of immersion, 50% of the soil in the 0.6% GG-modified loess was unslaked, while GG-modified loess with GG contents of 0.8% or higher still remained intact. The slaking process of GG-modified loess can likewise be divided into three stages: (1) the initial stage, during which distinct fissures developed on the surface of the sample with a GG content of 0.6%, whereas only a small number of air bubbles escaped from the surfaces of samples with other GG contents; (2) the intermediate stage, during which localized slaking occurred at the edges of the sample with a GG content of 0.6%, whereas fine fissures developed on the surfaces of samples with other GG contents, accompanied by slight surface uplift and localized bulging; and (3) the final stage, during which the samples were generally stable, with distinct slaking damage occurring only in the sample with a GG content of 0.6%, while the structures of samples with other GG contents remained intact. As shown in Fig. 5b, the slaking process of NS-modified loess was broadly similar to that of raw loess. However, with increasing NS content, the slaking volume of NS-modified loess at the same immersion time decreased. As shown in Fig. 5c, the slaking process of GG + NS composite-modified loess was similar to that of loess modified with 0.6% GG alone. Moreover, a higher GG content in the composite modifying material resulted in a smaller slaking volume of the modified loess.



(a)



(b)

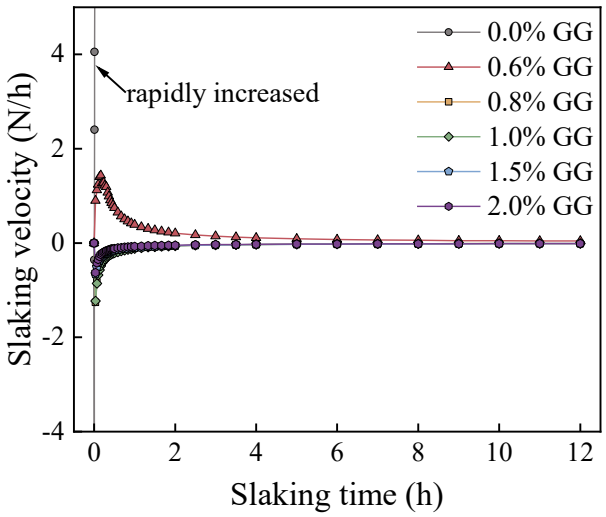


(c)

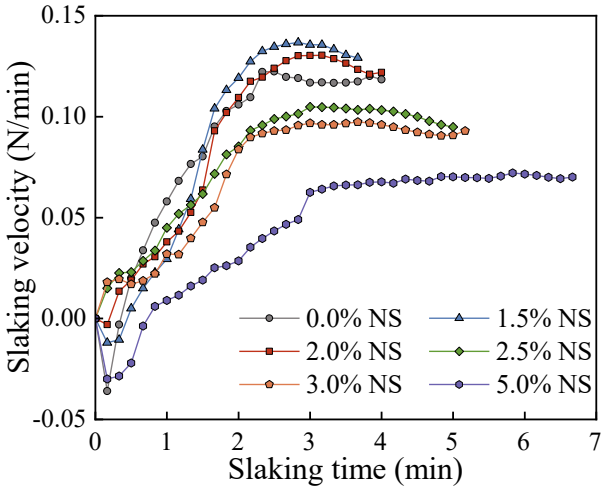
Fig. 6. Effects of different modifier contents on the slaking ratio of loess: (a) GG-modified loess; (b) NS-modified loess; (c) GG+NS composite-modified loess.

Figures 6 and 7 present the temporal variations in the slaking ratio and slaking rate of the modified loess, respectively. GG modification fundamentally improved the slaking resistance of loess. The final slaking ratio of loess modified with 0.6% GG, defined as the slaking ratio after 12 h of immersion, was 53%. When the GG content exceeded 0.8%, the final slaking ratio of the modified loess became negative. Combined with the slaking-rate results, this finding indicates that the loess gradually absorbed water and gained mass after immersion. At the end of the slaking test, the overall structure of the samples remained intact, with a final mass increase of approximately 14%. These results indicate that GG-modified loess exhibited significantly greater slaking resistance than raw

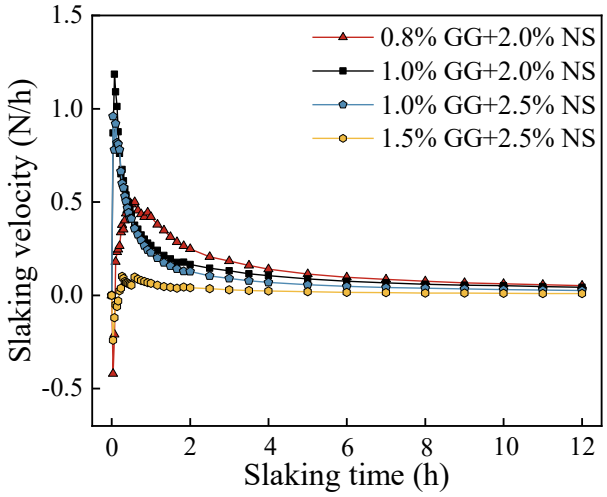
loess. NS incorporation did not fundamentally alter the slaking resistance of loess. Modified loess at all NS contents ultimately underwent complete slaking; however, increasing the NS content delayed the time required for complete slaking, from 240 s for raw loess to 400 s for loess modified with 5% NS. Notably, compared with raw loess, loess modified with 1.5% NS exhibited a higher slaking rate, a shorter time to complete slaking (220 s), and poorer slaking resistance. The improvement in loess slaking resistance produced by the composite modifying material was intermediate between those achieved using the two single modifying materials. The final slaking ratios of samples with all composite contents after 12 h ranged from 11.7% to 66.2%. These results indicate that NS addition weakened the improvement in loess slaking resistance induced by GG. Overall, the GG + NS composite modifying material significantly enhanced the slaking resistance of loess, although its modification effect was less pronounced than that of GG used alone.



(a)



(b)

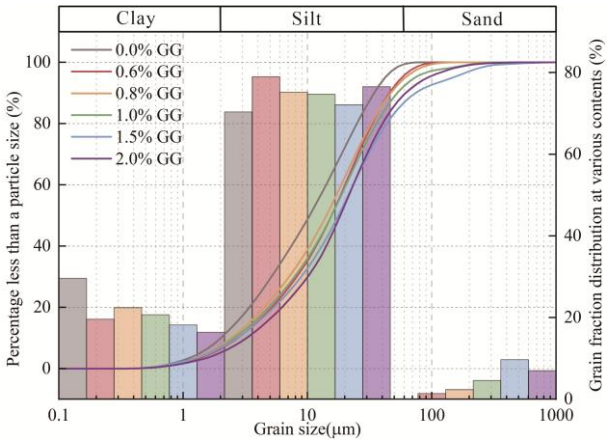


(c)

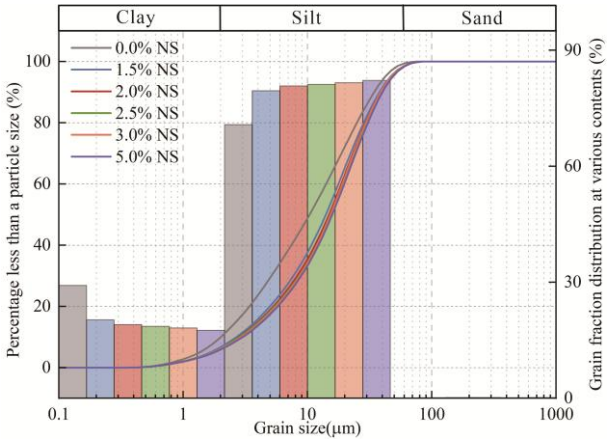
Fig. 7. Effects of different modifier contents on the slaking velocity of loess: (a) GG-modified loess; (b) NS-modified loess; (c) GG+NS composite-modified loess.

3.3 Basic Physical Property Characteristics

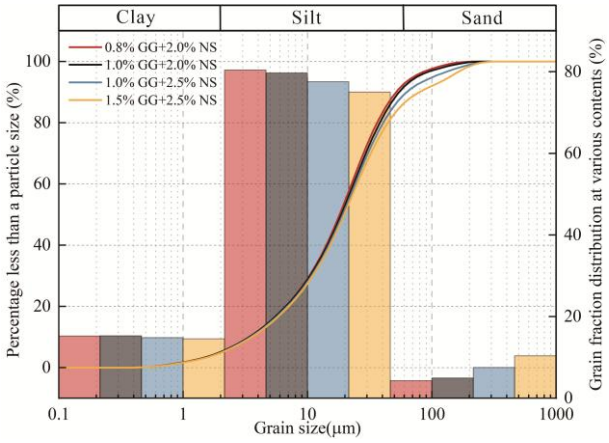
The results indicate that the incorporation of modifying materials effectively altered the particle-size distribution of loess, resulting in an overall coarsening of the soil particles. As shown in Fig. 8a, compared with raw loess, GG incorporation reduced the clay fraction (<0.005 mm) of the modified loess from 29.62% to 16.42%–22.44%, whereas both the silt fraction (0.005–0.075 mm) and sand fraction (0.075–2 mm) increased. Specifically, the silt fraction increased from 70.36% to 72.10%–78.99%, while the sand fraction increased from 0.02% to 1.40%–9.70%. As shown in Fig. 8b, as the NS content increased from 0% to 5%, the clay fraction of NS-modified loess gradually decreased from 20.29% to 17.60%, whereas the silt fraction gradually increased from 79.54% to 82.21%; no significant change was observed in the sand fraction. As shown in Fig. 8c, the clay fraction of GG + NS composite-modified loess changed only slightly. For loess modified with 0.8% GG + 2.0% NS, 1.0% GG + 2.0% NS, 1.0% GG + 2.5% NS, and 1.5% GG + 2.5% NS, the silt fractions were 80.42%, 79.72%, 77.57%, and 75.05%, respectively, whereas the corresponding sand fractions were 4.32%, 4.96%, 7.55%, and 10.40%. Compared with loess modified using GG or NS alone, the composite-modified loess exhibited lower clay and silt fractions and a markedly higher sand fraction.



(a)



(b)



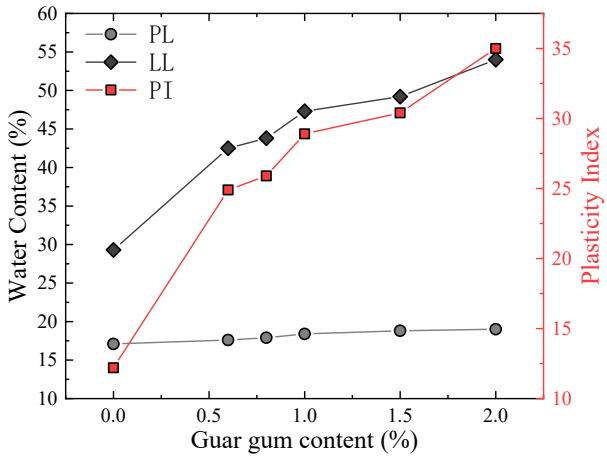
(c)

Fig. 8. Particle-size distribution curves of modified loess at different modifier contents: (a) GG-modified loess; (b) NS-modified loess; (c) GG+NS composite-modified loess.

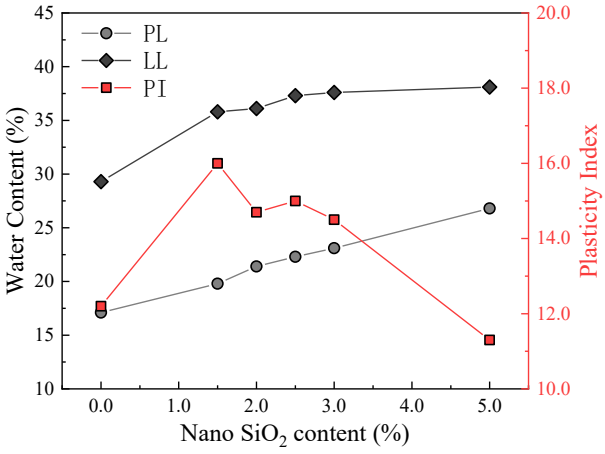
The liquid limit (LL), plastic limit (PL), and plasticity index (PI) of loess modified with the three materials at different contents are shown in Fig. 9. The modifying materials improved the water-related properties of loess, with both LL and PL increasing to varying degrees. GG incorporation

significantly increased the LL of loess, whereas its effect on PL was relatively limited. At GG contents of 0% (raw loess), 0.6%, 0.8%, 1.0%, 1.5%, and 2.0%, the LL values were 29.3%, 42.5%, 43.8%, 47.3%, 49.2%, and 54.0%, respectively, while the corresponding PL values were 17.1%, 17.6%, 17.9%, 18.4%, 18.8%, and 19.0%, respectively. The PI showed a marked increasing trend (Fig. 9a). NS incorporation increased both the LL and PL of loess. At NS contents of 0% (raw loess), 1.5%, 2.0%, 2.5%, 3.0%, and 5.0%, the LL values were 29.3%, 35.8%, 36.1%, 37.3%, 37.6%, and 38.1%, respectively, whereas the corresponding PL values were 17.1%, 19.8%, 21.4%, 22.3%, 23.1%, and 26.8%, respectively. The PI initially increased and subsequently decreased (Fig. 9b).

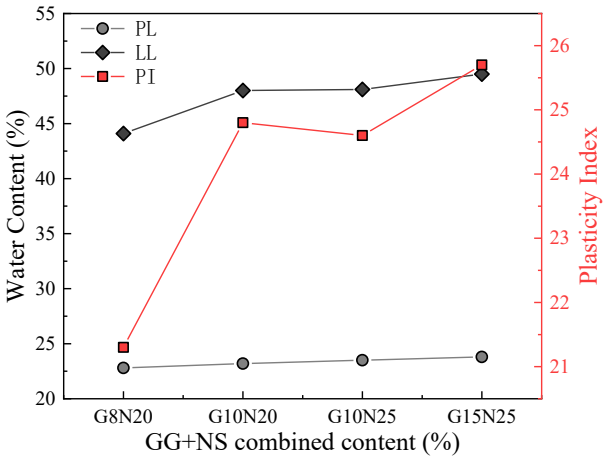
For composite-modified loess with contents of 0.8% GG + 2.0% NS, 1.0% GG + 2.0% NS, 1.0% GG + 2.5% NS, and 1.5% GG + 2.5% NS, the LL values were 44.1%, 48.0%, 48.1%, and 49.5%, respectively, while the corresponding PL values were 22.8%, 23.2%, 23.5%, and 23.8%, respectively. Compared with loess modified using GG or NS alone, the composite-modified loess exhibited higher liquid and plastic limits.



(a)



(b)



(c)

Fig. 9. Variations in liquid limit (LL), plastic limit (PL), and plasticity index (PI) of differently modified loess: (a) GG-modified loess; (b) NS-modified loess; (c) GG+NS composite-modified loess.

3.4 Micro–structural characteristics

Fig. 10 presents scanning electron microscopy (SEM) images of raw loess and loess samples incorporating different modifying materials at a magnification of 500×. The raw loess exhibited a loose structure, with interparticle contacts dominated by corner-to-corner and corner-to-edge contacts. The contact areas were small, and large interparticle pores were present (Fig. 10a). GG incorporation significantly improved the microstructure of loess. Upon contact with water, GG formed a flocculent gel-like substance with high adhesive strength. By cementing fine particles within the soil mass, filling interparticle pores, and coating soil particles, the GG increased the apparent particle size and reduced the pore area, resulting in a relatively dense loess structure (Fig. 10b). NS incorporation produced

different microstructural changes. NS was uniformly dispersed among the loess particles, filled interparticle pores, and partially formed small aggregates, thereby reducing the pore area (Fig. 10c).

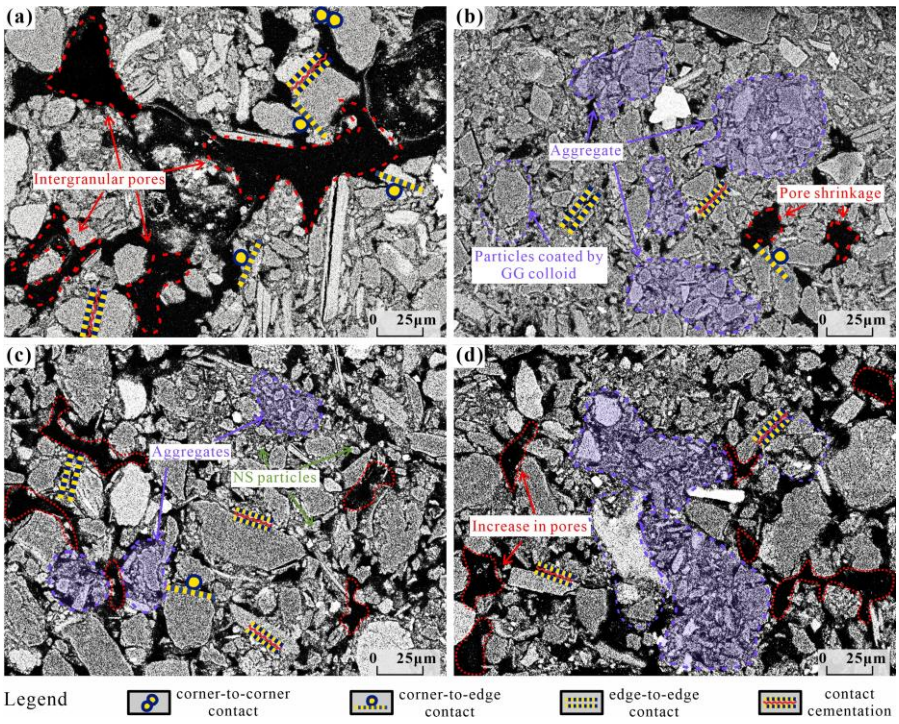
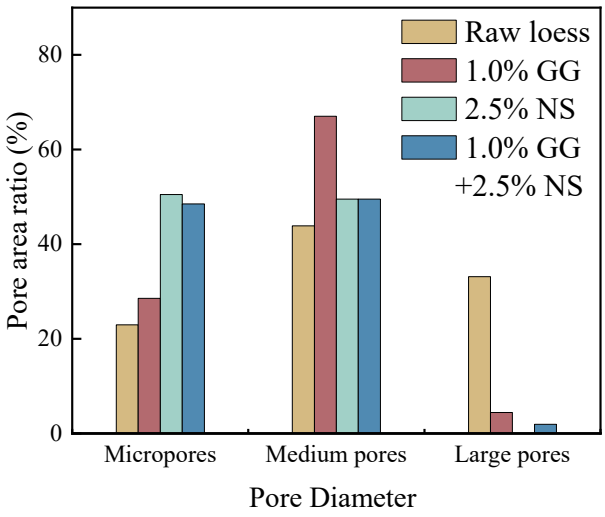


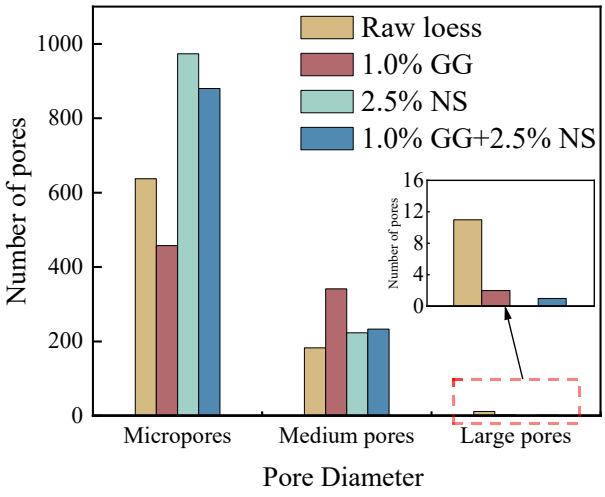
Fig. 10. Scanning Electron Microscope images: (a)Raw loess (b)GG-modified loess; (c) NS-modified loess; (d) GG+NS composite-modified loess.

Fig. 11 shows changes in the microscopic pore parameters of loess modified with different materials. GG incorporation substantially reduced the porosity of loess from 28% in raw loess to 14%. Specifically, the area fraction of large pores decreased markedly from 33% to 4%, whereas the area fractions of medium and small pores increased from 43% to 67% and from 23% to 29%, respectively (Fig. 11). For NS-modified loess, the porosity decreased from 28% in raw loess to 20%. The area fraction of large pores decreased from 33% to 0%, whereas those of medium and small pores increased from 44% to 50% and from 23% to 50%, respectively (Fig. 11a, b). When GG and NS were incorporated together, the porosity of the composite-modified loess was 19.84%. The area fractions and numbers of pores of all size categories were intermediate between the corresponding values for loess modified with GG alone and NS alone. These results indicate that GG and NS exerted both complementary and counteracting effects on loess modification.



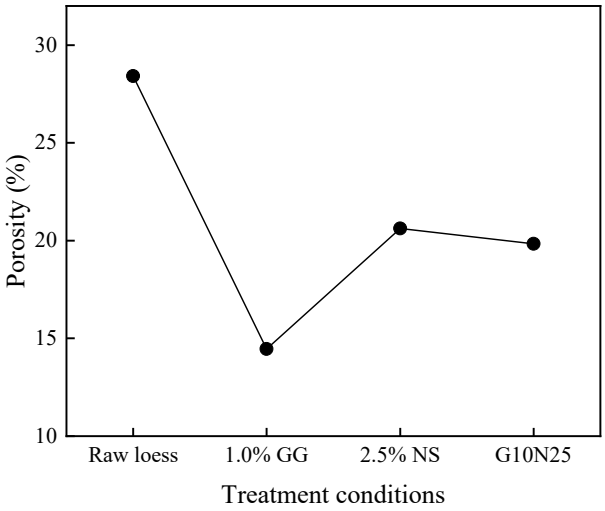
309

310 （a）



311

312 （b）



313

314 （c）

315 **Fig. 11.** Pore parameters of differently modified loess specimens:(a) pore area ratio; (b) number of

pores; (c) Porosity

4. Discussion

4.1 Mechanical Strength Enhancement Mechanisms of Modified Loess

During direct shear testing of loess, normal pressure drives soil particles to fill pore spaces. Sustained unidirectional shear stress subsequently induces rotation of the long axes of soil particles in the vicinity of the shear band, ultimately resulting in a preferred orientation parallel to the shear plane [34] (Fig. 12c).

GG incorporation significantly enhanced the shear strength of loess. On the one hand, after incorporation into loess, GG undergoes hydration with pore water to form a hydrogel [19]. On the other hand, GG is a nonionic polysaccharide rich in hydroxyl groups [35]. Its hydroxyl groups can form high-energy hydrogen bonds with exposed oxygen atoms in Si–O groups and other functional groups on the surfaces of clay minerals in loess [31], thereby linking soil particles to the gel phase [36]. Through the synergistic action of these two mechanisms (Fig. 12b), a continuous three-dimensional cementation network is formed within the GG-modified loess. This network constrains the movement and rotation of soil particles during shearing, thereby enhancing the shear strength of GG-modified loess [26]. However, the development of this cementation network is spatially constrained within the soil mass. Excessive GG incorporation forms thicker hydrogel layers between soil particles and increases the interparticle spacing, thereby weakening the modification effect of GG. This effect is reflected in the decrease in loess shear strength at GG contents of 1.5% and 2.0%. In addition, the cohesion of GG-modified loess increased substantially, whereas the friction angle changed only slightly. This is because the three-dimensional GG gel network cemented soil particles through hydrogen bonding, constrained their relative displacement, and markedly increased cohesion [12, 23].

NS incorporation substantially enhanced the shear strength of loess. On the one hand, owing to their nanoscale size, NS particles can effectively fill micropores in loess [27]. This process reduces the proportion of large and medium pores, divides them into a greater number of smaller pores, and decreases the overall porosity of loess [37]. On the other hand, microaggregates form within NS-modified loess. When loess and NS are mixed with water, Ca^{2+} and Mg^{2+} ions are released. These ions can replace K^{+} and Na^{+} ions on the surfaces of clay particles, thereby reducing the thickness of the

diffuse double layer and the bound-water film surrounding the clay particles. Consequently, the interparticle distance decreases and the van der Waals attraction between particles is substantially enhanced [25]. In addition, NS particles react with Ca^{2+} in soil pores through pozzolanic reactions, generating C–S–H gel in situ [28, 38]. These mechanisms substantially enhance the van der Waals attraction within loess. Consequently, NS modification exerts a more pronounced effect on cohesion than on the friction angle. Notably, Ca^{2+} is derived mainly from natural calcium carbonate and soluble calcareous cementing materials in loess [39], both of which occur at relatively low contents; therefore, the effect of the generated C–S–H gel is limited [40].

The GG + NS composite modifying material enhanced the shear strength of loess more effectively than either modifying material used alone, which can be attributed to the synergistic and complementary mechanisms of GG and NS (Fig. 12d). GG primarily fills macropores and forms a continuous three-dimensional cementation network within the loess, whereas nanoscale NS particles fill micropores within the GG-cemented network, thereby producing a more intact loess structure.

4.2 Slaking Resistance Enhancement Mechanisms of Modified Loess

The slaking resistance of loess is primarily governed by the degree of attenuation of interparticle cementation upon wetting and by its pore structure. The cementation provided by soluble salts and organic matter in raw loess exhibits poor water stability and readily dissolves upon contact with water [33]. Meanwhile, the highly porous structure of raw loess provides pathways for rapid water infiltration and readily induces an intense water–air displacement effect. During gas escape, the resulting air pressure disrupts the surrounding soil skeleton, induces new fissures, and entrains some soil particles [41], ultimately leading to loess slaking (Fig. 12e).

The enhanced slaking resistance of GG-modified loess results from the blockage of water-infiltration pathways by its three-dimensional cementation structure, together with the favorable impermeability and water stability of the hydrogel itself [14]. Although hydration causes moderate gel softening, the cemented framework is not readily disrupted and can effectively resist water erosion while maintaining the structural integrity of the loess (Fig. 12f). The slaking-test results show that loess modified with 0.6% GG exhibited lower slaking resistance than loess modified with higher GG contents (Fig. 5a). This is because the three-dimensional gel network formed at a low GG content did not

completely fill the pores of the loess. Following immersion, water could still infiltrate the soil mass through unblocked pathways, ultimately causing uncemented soil particles to detach. The improvement in loess slaking resistance induced by NS is mainly attributable to the reduction in water-flow pathways through NS filling and to the cementation provided by C–S–H gel between soil particles. However, because only trace amounts of C–S–H gel are generated within the loess, NS provides only limited improvement in loess slaking resistance.

In terms of slaking resistance, GG + NS composite-modified loess performed better than raw loess and loess modified with NS alone but worse than loess modified with GG alone. This phenomenon occurs because the competitive adsorption of NS particles weakens the cementation effect of GG. Consequently, some soil particles within the soil mass are not cemented by GG, preventing the formation of a complete GG-cemented network structure. Water can then infiltrate the soil through pores that are not cemented by GG, inducing localized softening and slaking as well as fissure propagation, and ultimately causing the soil mass to gradually slake along its edge pores (Fig. 12f).

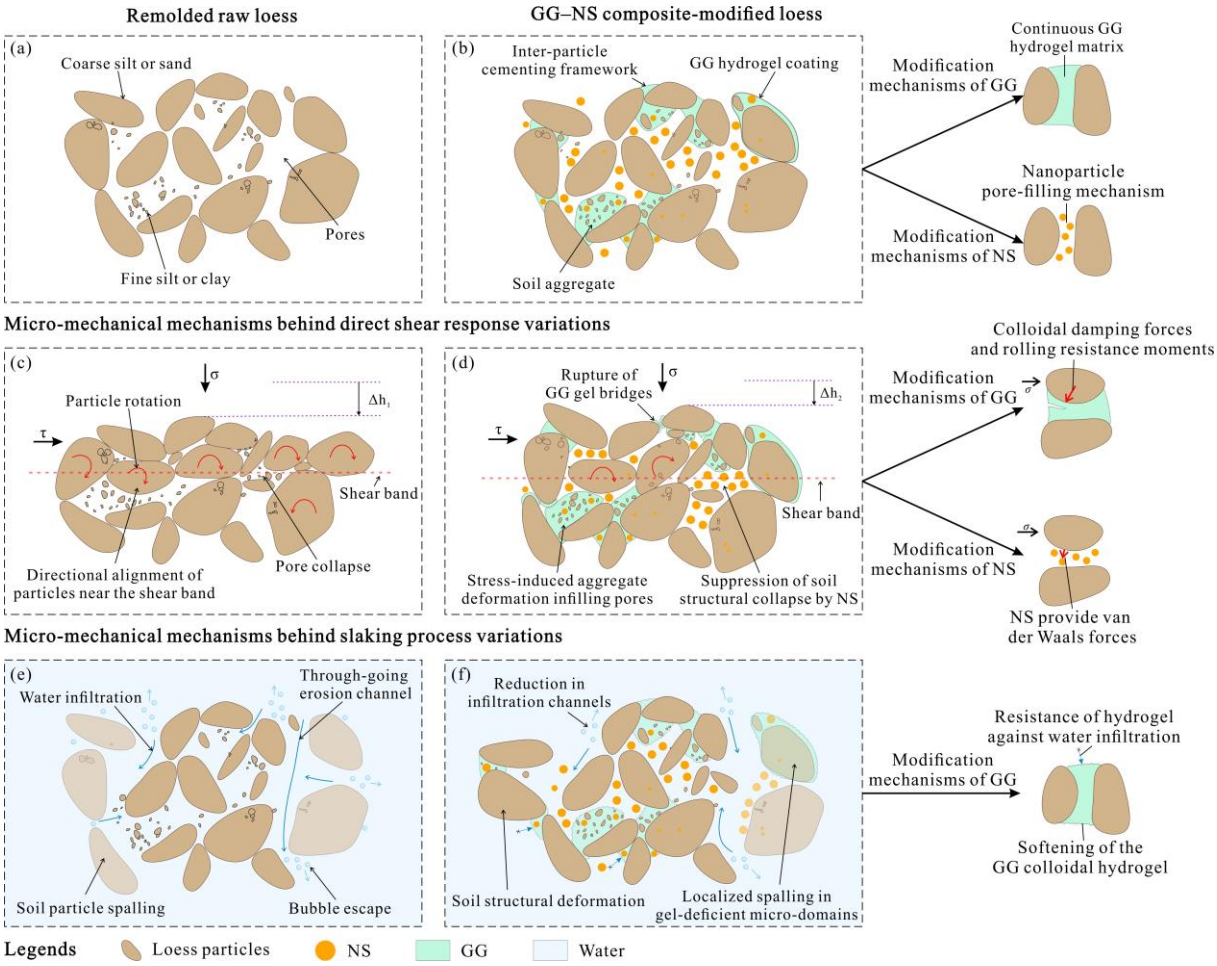


Fig. 12. Schematic diagram of the microscopic reinforcement mechanisms of modified loess

4.3 Comparison of present and previous studies

Table. 3 compares the results of the present study with those reported in previous studies. Li [26] investigated the effects of lignin and GG on the mechanical properties and water stability of loess through direct shear and slaking tests. Their results showed that GG incorporation alone increased the shear strength of loess, primarily owing to a substantial increase in cohesion. In addition, lignin incorporation enhanced the shear strength of GG-modified loess but adversely affected its slaking resistance.

Cui [42] and Changizi and Haddad [43] investigated the effects of composite materials containing nano-SiO_2 on the mechanical properties of soil through direct shear tests. Their results showed that the shear strength of the modified soil increased with increasing nano-SiO_2 content. Furthermore, the composite materials improved soil shear strength more effectively than the individual modifying materials.

The GG + NS composite material significantly improved both the shear strength and slaking resistance of loess. Within the composite, GG primarily contributed to improving loess slaking resistance, whereas NS predominantly enhanced its mechanical properties. In the present study, the GG + NS composite increased the cohesion and friction angle of loess by 249.8% and 17.2%, respectively. Li [26] reported that a lignin + guar gum composite increased the friction angle of loess by 12.6% but decreased its cohesion by 7.4%. Therefore, the GG + NS composite developed in the present study provided a greater enhancement in loess shear strength than the lignin + GG composite.

Comparison with the results reported by Cui [42] and Changizi and Haddad [43] indicated that the shear-strength enhancement achieved by the GG + NS composite in the present study was intermediate between those reported in these two studies. However, loess modified with the GG + NS composite did not undergo complete slaking after 12 h of immersion, demonstrating its substantial improvement in loess slaking resistance.

Notably, both the present study and Cui [42] showed that NS exerted a more pronounced effect on cohesion than on the friction angle. In contrast, Changizi and Haddad [43] reported that, for NS-modified clay, the friction angle contributed more effectively to strength enhancement than cohesion. This discrepancy may be attributed to differences in the clay fraction of the soils used in these studies [37].

5. Conclusion

This study used guar gum (GG) and nano- SiO_2 (NS) as modifying materials, with their contents as the experimental variables. Systematic tests were conducted to evaluate the macroscopic mechanical properties of loess, including shear strength and slaking resistance. Particle-size analysis, Atterberg-limit tests, and scanning electron microscopy (SEM) analysis were further performed to elucidate the effects of GG and NS on the mechanical strength and water stability of loess. The main conclusions are as follows:

(1) Both GG and NS positively enhanced the shear strength of loess, and the shear strength of GG + NS composite-modified loess exceeded that of loess modified with either material alone. Loess modified with 1.0% GG + 2.5% NS exhibited the optimal performance. Under a normal pressure of 200 kPa, its shear strength was 36.7% and 8.5% higher than that of loess modified with 1.0% GG alone and 2.5% NS alone, respectively.

(2) The slaking behavior of GG-modified loess and GG + NS composite-modified loess was markedly altered, with evident improvement in slaking resistance. Loess modified with GG contents of 0.8% or higher remained intact after 12 h of immersion. Among the composite formulations, loess modified with 1.5% GG + 2.5% NS exhibited the highest slaking resistance, with a final slaking ratio of 11.7%.

(3) Compared with raw loess, the incorporation of modifying materials increased the particle size of loess. GG modification significantly increased the LL, whereas its effect on the PL was limited. NS modification increased both the LL and PL to some extent. In addition, compared with loess modified using either material alone, GG + NS composite-modified loess exhibited higher LL and PL values.

(4) The incorporation of modifying materials significantly improved the microstructure of loess. Compared with raw loess, the porosity of GG-modified loess decreased to 14%, whereas those of NS-modified loess and GG + NS composite-modified loess decreased to 20% and 19%, respectively.

(5) The GG + NS composite material exhibits both synergistic and counteracting effects in loess. On the one hand, GG provides a networked cementation structure that maintains the soil skeleton and increases interparticle cementation, whereas NS fills micropores and improves structural integrity. Their synergistic effects enable the composite-modified loess to achieve greater shear strength than loess modified with either material alone. On the other hand, NS particles competitively weaken the continuity of the GG gel network, causing progressive spalling of localized soil regions not cemented by GG during slaking. Consequently, the slaking resistance of composite-modified loess is lower than that of loess modified with GG alone.

Considering engineering cost, the effect on loess brittleness, and improvements in the mechanical properties and water stability of loess, 1.0% and 2.5% are recommended as the optimal contents of GG and NS, respectively. The optimal formulation for composite-modified loess is 1.0% GG + 2.5% NS.

Data availability

The datasets used and analysed during the current study available from the corresponding author on reasonable request.

Reference

1 Yang, J. *et al.* Experimental investigations on the physico-mechanical and microstructural properties of loess reinforced with anionic polyacrylamide. *Construction and Building Materials* **409**, 134124, doi:10.1016/j.conbuildmat.2023.134124 (2023).

2 Carey, J. M., McSaveney, M. J. & Petley, D. N. Dynamic liquefaction of shear zones in intact loess during simulated earthquake loading. *Landslides* **14**, 789-804, doi:10.1007/s10346-016-0746-y (2017).

3 Li, Y. A review of shear and tensile strengths of the Malan Loess in China. *Engineering Geology* **236**, 4-10, doi:10.1016/j.enggeo.2017.02.023 (2018).

4 4 Kim, Y., Park, H. & Jeong, S. Settle ment Behavior of Shallow Foundations in Unsaturated Soils under Rainfall. *Sustainability* **9**, 1417, doi:10.3390/su9081417 (2017).

5 Jie, Y.-x., Wei, Y.-j., Wang, D.-l. & Wei, Y.-f. Numerical study on settlement of high-fill airports in collapsible loess geomaterials: A case study of Lüliang Airport in Shanxi Province, China. *Journal of Central South University* **28**, 939-953, doi:10.1007/s11771-021-4655-4 (2021).

6 Zhou, Y. F., Tham, L. G., Yan, W. M., Dai, F. C. & Xu, L. Laboratory study on soil behavior in loess slope subjected to infiltration. *Engineering Geology* **183**, 31-38, doi:10.1016/j.enggeo.2014.09.010 (2014).

7 Leng, Y., Peng, J., Wang, Q., Meng, Z. & Huang, W. A fluidized landslide occurred in the Loess Plateau: A study on loess landslide in South Jingyang tableland. *Engineering Geology* **236**, 129-136, doi:10.1016/j.enggeo.2017.05.006 (2018).

8 Peng, J. *et al.* The critical issues and creative concepts in mitigation research of loess geological hazards (in chinese). *Journal of Engineering Geology* **22**, 684-691, doi:10.13544/j.cnki.jeg.2014.04.014 (2014).

9 Khodabandeh, M. A., Nagy, G. & Török, Á. Stabilization of collapsible soils with nanomaterials, fibers, polymers, industrial waste, and microbes: Current trends. *Construction and Building Materials* **368**, 130463, doi:10.1016/j.conbuildmat.2023.130463 (2023).

10 Nwonu, D. C. Exploring soil geopolymer technology in soft ground improvement: a brief excursion. *Arabian Journal of Geosciences* **14**, doi:10.1007/s12517-021-06832-x (2021).

11 Chang, I. *et al.* Review on biopolymer-based soil treatment (BPST) technology in geotechnical engineering practices. *Transportation Geotechnics* **24**, 100385, doi:10.1016/j.trgeo.2020.100385 (2020).

12 Ayeldeen, M., Negm, A., El-Sawwaf, M. & Kitazume, M. Enhancing mechanical behaviors of collapsible soil using two biopolymers. *Journal of Rock Mechanics and Geotechnical Engineering* **9**, 329-339, doi:10.1016/j.jrmge.2016.11.007 (2017).

13 Ayeldeen, M. K., Negm, A. M. & El Sawwaf, M. A. Evaluating the physical characteristics of biopolymer/soil mixtures. *Arabian Journal of Geosciences* **9**, doi:10.1007/s12517-016-2366-1 (2016).

14 Dehghan, H., Tabarsa, A., Latifi, N. & Bagheri, Y. Use of xanthan and guar gums in soil strengthening. *Clean Technologies and Environmental Policy* **21**, 155-165, doi:10.1007/s10098-018-1625-0 (2019).

15 Ghasabkolaei, N., Janalizadeh Choobbasti, A., Roshan, N. & Ghasemi, S. E. Geotechnical properties of the soils modified with nanomaterials: A comprehensive review. *Archives of Civil and Mechanical Engineering* **17**, 639-650, doi:10.1016/j.acme.2017.01.010 (2017).

16 Huang, Y. & Wang, L. Experimental studies on nanomaterials for soil improvement: a review. *Environmental Earth Sciences* **75**, doi:10.1007/s12665-015-5118-8 (2016).

17 Changizi, F. & Haddad, A. Improving the geotechnical properties of soft clay with nano-silica particles. *Proceedings of the Institution of Civil Engineers - Ground Improvement* **170**, 62-71, doi:10.1680/jgrim.15.00026 (2017).

18 Haeri, S. M. & Valishzadeh, A. Evaluation of Using Different Nanomaterials to Stabilize the Collapsible Loessial Soil. *International Journal of Civil Engineering* **19**, 583-594, doi:10.1007/s40999-020-00583-8 (2020).

19 Xu, X. *et al.* Dispersion, mechanical, hydrophysical properties and mechanistic analysis of improved dispersive soil using guar gum. *Bulletin of Engineering Geology and the Environment* **84**, 1-19, doi:10.1007/s10064-024-04082-1 (2025).

20 Kholghifard, M. & Amini Behbahani, B. Shear strength of clayey sand treated by nanoclay mixed with recycled polyester fiber. *Journal of Central South University* **29**, 259-269,

509 doi:10.1007/s11771-022-4895-y (2022).
510 21 Kulanthaivel, P., Selvakumar, S., Soundara, B., Kayalvizhi, V. S. & Bhuvaneshwari, S. Combined
511 effect of nano-silica and randomly distributed fibers on the strength behavior of clay soil.
512 *Nanotechnology for Environmental Engineering* **7**, 23-34, doi:10.1007/s41204-021-00176-3
513 (2022).
514 22 Onah, H. N., Nwonu, D. C. & Ikeagwuani, C. C. Feasibility of lime and biopolymer treatment for
515 soft clay improvement: a comparative and complementary approach. *Arabian Journal of*
516 *Geosciences* **15**, 1-19, doi:10.1007/s12517-022-09552-y (2022).
517 23 Fu, H.-Y., Yu, G.-T., Gao, Q.-F., Zeng, L. & Cao, S.-P. Crack Resistance and Strength Properties
518 of Red Clay Modified with Lignocellulose and Guar Gum. *KSCE Journal of Civil Engineering*
519 **27**, 4152-4162, doi:10.1007/s12205-023-2005-9 (2023).
520 24 Rong, X. *et al.* Mechanical behavior and strengthening mechanism of loess stabilized with
521 xanthan gum and guar gum biopolymers. *Materials Research Express* **11**, 105305,
522 doi:10.1088/2053-1591/ad832c (2024).
523 25 Wang, L. *et al.* Effect of nanosilica on the hydrological properties of loess and the microscopic
524 mechanism. *Scientific Reports* **14**, 13692, doi:10.1038/s41598-024-64280-5 (2024).
525 26 Li, Z. *et al.* Comprehensive performance tests and evaluations of the slope protection effect of
526 lignin and guar gum-modified loess. *Bulletin of Engineering Geology and the Environment* **85**,
527 doi:10.1007/s10064-026-04927-x (2026).
528 27 Kong, R., Zhang, F., Wang, G. & Peng, J. Stabilization of Loess Using Nano-SiO(2). *Materials*
529 *(Basel)* **11**, doi:10.3390/ma11061014 (2018).
530 28 Choobbasti, A. J. & Kutanaei, S. S. Microstructure characteristics of cement-stabilized sandy soil
531 using nanosilica. *Journal of Rock Mechanics and Geotechnical Engineering* **9**, 981-988,
532 doi:10.1016/j.jrmge.2017.03.015 (2017).
533 29 Gao, J. *et al.* Study on Treatment of Loess Landslide Based on Nanosilica and Fly Ash Composite
534 Stabilizer Filling Fissures. *Advances in Civil Engineering* **2020**, 8884981,
535 doi:10.1155/2020/8884981 (2020).
536 30 Babaei, A., Ghazavi, M. & Ganjian, N. Shear Strength Parameters of Clayey Sand Treated with

Cement and Nano Titanium Dioxide. *Geotechnical and Geological Engineering* **40**, 133-151, doi:10.1007/s10706-021-01881-1 (2022).

31 Sujatha, E. R. & Saisree, S. Geotechnical behaviour of guar gum-treated soil. *Soils and Foundations* **59**, 2155-2166, doi:10.1016/j.sandf.2019.11.012 (2019).

32 Duan, Z. *et al.* Characteristics and mechanisms of soil structure damage under salt weathering. *Soil and Tillage Research* **238**, 106030, doi:10.1016/j.still.2024.106030 (2024).

33 Li, X. a., Huang, R. & Peng, J. Experimental research on disintegration of loess (in chinese). *Chinese Journal of Rock Mechanics and Engineering* **28**, 3207-3213, doi:10.3321/j.issn:1000-6915.2009.z1.092 (2009).

34 Yuan, W., Fan, W., Deng, L., Li, W. & Zhou, Y. Particle structure characteristics of loess and their effects on shear behavior (in chinese). *Journal of Engineering Geology* **29**, 871-878, doi:10.13544/j.cnki.jeg.2021-0255 (2021).

35 Sharma, G. *et al.* Guar gum and its composites as potential materials for diverse applications: A review. *Carbohydrate Polymers* **199**, 534-545, doi:10.1016/j.carbpol.2018.07.053 (2018).

36 Anandha Kumar, S. & Sujatha, E. R. An appraisal of the hydro-mechanical behaviour of polysaccharides, xanthan gum, guar gum and beta-glucan amended soil. *Carbohydrate Polymers* **265**, 118083, doi:10.1016/j.carbpol.2021.118083 (2021).

37 Aksu, G. & Eskisar, T. The geomechanical properties of soils treated with nanosilica particles. *Journal of Rock Mechanics and Geotechnical Engineering* **15**, 954-969, doi:10.1016/j.jrmge.2022.06.013 (2023).

38 Masrour, F. F., Mirsadeghi, M. N., MolaAbasi, H. & Chenari, R. J. Effect of Nanosilica on the Macro- and Microbehavior of Dispersive Clays. *Journal of Materials in Civil Engineering* **33**, 04021349, doi:10.1061/(asce)mt.1943-5533.0003975 (2021).

39 Huang, T. & Ma, B. The Origin of Major Ions of Groundwater in a Loess Aquifer. *Water* **11**, 2464, doi:10.3390/w11122464 (2019).

40 Bahmani, S. H., Huat, B. B. K., Asadi, A. & Farzadnia, N. Stabilization of residual soil using SiO2 nanoparticles and cement. *Construction and Building Materials* **64**, 350-359, doi:10.1016/j.conbuildmat.2014.04.086 (2014).

41 Caron, J., Espindola, C. R. & Angers, D. A. Soil Structural Stability during Rapid Wetting: Influence of Land Use on Some Aggregate Properties. *Soil Science Society of America Journal* **60**, 901-908, doi:10.2136/sssaj1996.03615995006000030032x (1996).

42 Cui, H., Jin, Z., Bao, X., Tang, W. & Dong, B. Effect of carbon fiber and nanosilica on shear properties of silty soil and the mechanisms. *Construction and Building Materials* **189**, 286-295, doi:10.1016/j.conbuildmat.2018.08.181 (2018).

43 Changizi, F. & Haddad, A. Strength properties of soft clay treated with mixture of nano-SiO2 and recycled polyester fiber. *Journal of Rock Mechanics and Geotechnical Engineering* **7**, 367-378, doi:10.1016/j.jrmge.2015.03.013 (2015).

Acknowledgments

This study would not have been possible without financial support from the Special Fund for the National Natural Science Foundation of China under Grant No. 42177155.

Author contributions

Conceptualization: Zhao Duan; Data curation: Shunxin Zhang, Xinyan Xie; Formal analysis: Shunxin Zhang, Xinyan Xie; Funding acquisition: Zhao Duan, Zhe Yang; Investigation Zhao: Duan Shunxin Zhang, Xinyan Xie, Zhuo Nan; Methodology: Zhao Duan, Zhe Yang; Project administration: Zhao Duan, Zhuo Nan; Resources: Zhao Duan, Zhe Yang; Software: Shunxin Zhang, Zhuo Nan; Supervision: Zhao Duan, Xinyan Xie, Zhe Yang; Validation: Xinyan Xie, Zhe Yang; Visualization: Shunxin Zhang, Xinyan Xie; Writing—original draft: Shunxin Zhang; Writing—review & editing: Zhao Duan, Shunxin Zhang. All authors have read and agreed to the published version of the manuscript.

Funding

This study was supported by the National Natural Science Foundation of China (No. 42177155).

Additional Information

Competing interests

The authors declare no competing interests.

Figure legends

Fig. 1. Specimen Preparation and Testing Apparatus.

Fig. 2. Stress-strain curves of loess treated with different modifiers (σ = 200 kPa): (a) GG-modified

loess; (b) NS-modified loess; (c) GG+NS composite-modified loess.

Fig. 3. Effect of modifier content on the peak shear strength under various normal stresses: (a) GG-modified loess; (b) NS-modified loess; (c) GG+NS composite-modified loess.

Fig. 4. Variations in shear strength parameters (c and φ) of modified loess with different modifier contents: (a) GG-modified loess; (b) NS-modified loess; (c) GG+NS composite-modified loess.

Fig. 5. Slaking process of differently modified loess specimens: (a) GG-modified loess; (b) NS-modified loess; (c) GG+NS composite-modified loess.

Fig. 6. Effects of different modifier contents on the slaking ratio of loess: (a) GG-modified loess; (b) NS-modified loess; (c) GG+NS composite-modified loess.

Fig. 7. Effects of different modifier contents on the slaking velocity of loess: (a) GG-modified loess; (b) NS-modified loess; (c) GG+NS composite-modified loess.

Fig. 8. Particle-size distribution curves of modified loess at different modifier contents: (a) GG-modified loess; (b) NS-modified loess; (c) GG+NS composite-modified loess.

Fig. 9. Variations in liquid limit (LL), plastic limit (PL), and plasticity index (PI) of differently modified loess: (a) GG-modified loess; (b) NS-modified loess; (c) GG+NS composite-modified loess.

Fig. 10. Scanning Electron Microscope images: (a)Raw loess (b)GG-modified loess; (c) NS-modified loess; (d) GG+NS composite-modified loess.

Fig. 11. Pore parameters of differently modified loess specimens:(a) pore area ratio; (b) number of pores; (c) Porosity

Fig. 12. Schematic diagram of the microscopic reinforcement mechanisms of modified loess

Tables

Table. 1. Basic physical properties of the loess samples used in the experiment

Physical parameter	Value	Method	Standard
Natural water content, ω (%)	15.5	Mass	ASTM D2216
Dry density, ρd (g/cm3)	1.55	Compaction	ASTM D1557
Void ratio, e	0.74	Not available	Not available
Specific gravity, GS	2.7	Water pycnometer	ASTM D854
Liquid limit, ωL	29.3	Wet prep	ASTM D4318
Plastic limit, ωP	17.1	Wet prep	ASTM D4318
Plasticity index, IP	12.2	Wet prep	ASTM D4318

615 **Table. 2.** Experimental scheme

Specimen ID		Content of GG (%)	Content of NS (%)	Specimen batch size			
				Direct shear test	Slaking test	Basic physical property test	SEM test
A：Raw loess	S0	0	0	3	1	1	1
B：GG-modified loess	G6	0.6	0	3	1	1	/
	G8	0.8		3	1	1	/
	G10	1		3	1	1	1
	G15	1.5		3	1	1	/
	G20	2		3	1	1	/
C：NS-modified loess	N15	0	1.5	3	1	1	/
	N20		2	3	1	1	/
	N25		2.5	3	1	1	1
	N30		3	3	1	1	/
	N50		5	3	1	1	/
D：GG+NS composite-modified loess	G8N20	0.8	2	3	1	1	/
	G10N20	1	2	3	1	1	/
	G10N25	1	2.5	3	1	1	1
	G15N25	1.5	2.5	3	1	1	/
Total sample size	/	/	/	48	16	16	4

616

617 **Table. 3.** Comparisons between previous studies and present study

Data sources	Soil	Stabilizer and content	Shear strength variation behavior		Anti-slaking behavior
			Cohesion	Friction angle	
Li et al [26]	Loess	2% GG	+35.3%	+4.1%	Slaking percentage: 1.5%
		2% GG + 2% Lignin	-7.4%	+12.6%	Slaking percentage: 2.4%
Cui et al [42]	Silt	3% NS	+117%	+1.6%	/
		3% NS + 2% Carbon fiber	+13478.9%	+11.8%	/
Changizi et al [43]	Clay	1.0% NS	+1.84%	+118.2%	/
		1.0% NS + 0.5% fiber	+197.3%	+185.2%	/
Present study	Loess	1 % GG	+88.3%	+3.8%	Slaking percentage: -10%
		2.5% NS	+226.5%	-8.7%	The sample completely slaked after 300 s
		1 % GG + 2.5% NS	+249.8%	+17.2%	Slaking percentage: 31%

618 **Note:** Data under "Shear strength variation behavior" represent the percentage increase in the shear
619 strength parameters of modified loess relative to untreated loess; the slaking rate denotes the mass
620 percentage of the soil specimen that disintegrated upon reaching relative stability.
621